



TIME WAITS FOR NO ONE

Enlist the experts at Bio X Cell for  
Antibody Production Services

EXPLORE

RECEIVE 10% OFF NOW with code: CONTRACT22JI



This information is current as  
of February 26, 2022.

## Cutting Edge: IFN- $\beta$ Expression in the Spleen Is Restricted to a Subpopulation of Plasmacytoid Dendritic Cells Exhibiting a Specific Immune Modulatory Transcriptome Signature

Jens Bauer, Regine J. Dress, Anja Schulze, Philipp Dresing, Shafaqat Ali, René Deenen, Judith Alferink and Stefanie Scheu

*J Immunol* 2016; 196:4447-4451; Prepublished online 2 May 2016;

doi: 10.4049/jimmunol.1500383

<http://www.jimmunol.org/content/196/11/4447>

**Supplementary Material** <http://www.jimmunol.org/content/suppl/2016/04/30/jimmunol.1500383.DCSupplemental>

**References** This article **cites 17 articles**, 8 of which you can access for free at:  
<http://www.jimmunol.org/content/196/11/4447.full#ref-list-1>

**Why *The JI*? Submit online.**

- **Rapid Reviews! 30 days\*** from submission to initial decision
- **No Triage!** Every submission reviewed by practicing scientists
- **Fast Publication!** 4 weeks from acceptance to publication

*\*average*

**Subscription** Information about subscribing to *The Journal of Immunology* is online at:  
<http://jimmunol.org/subscription>

**Permissions** Submit copyright permission requests at:  
<http://www.aai.org/About/Publications/JI/copyright.html>

**Email Alerts** Receive free email-alerts when new articles cite this article. Sign up at:  
<http://jimmunol.org/alerts>



# Cutting Edge: IFN- $\beta$ Expression in the Spleen Is Restricted to a Subpopulation of Plasmacytoid Dendritic Cells Exhibiting a Specific Immune Modulatory Transcriptome Signature

Jens Bauer,<sup>\*,1</sup> Regine J. Dress,<sup>\*,1</sup> Anja Schulze,<sup>\*</sup> Philipp Dresing,<sup>\*</sup> Shafaqat Ali,<sup>\*</sup> René Deenen,<sup>†</sup> Judith Alferink,<sup>‡,§</sup> and Stefanie Scheu<sup>\*</sup>

Type I IFNs are critical in initiating protective antiviral immune responses, and plasmacytoid dendritic cells (pDCs) represent a major source of these cytokines. We show that only few pDCs are capable of producing IFN- $\beta$  after virus infection or CpG stimulation. Using IFN $\beta$ /YFP reporter mice, we identify these IFN- $\beta$ -producing cells in the spleen as a CCR9<sup>+</sup>CD9<sup>+</sup> pDC subset that is localized exclusively within the T/B cell zones. IFN- $\beta$ -producing pDCs exhibit a distinct transcriptome profile, with higher expression of genes encoding cytokines and chemokines, facilitating T cell recruitment and activation. These distinctive characteristics of IFN- $\beta$ -producing pDCs are independent of the type I IFNR-mediated feedback loop. Furthermore, IFN- $\beta$ -producing pDCs exhibit enhanced CCR7-dependent migratory properties in vitro. Additionally, they effectively recruit T cells in vivo in a peritoneal inflammation model. We define “professional type I IFN-producing cells” as a distinct subset of pDCs specialized in coordinating cellular immune responses. *The Journal of Immunology*, 2016, 196: 4447–4451.

**E**arly type I IFN expression is crucial for the initiation of antiviral immune responses. A primary source of type I IFNs is plasmacytoid dendritic cells (pDCs), which rapidly produce large amounts of these cytokines upon activation (1, 2) and, therefore, have been termed professional type I IFN producers. In general, pDCs are identified based on their specific surface marker expression profile as CD11c<sup>int</sup>B220<sup>+</sup>mPDCA-1<sup>+</sup>CD11b<sup>+</sup>, but they represent a rather heterogeneous cell population. Functionally separate subsets of pDCs have been described based on the expression of CD9 versus CCR9. In the bone marrow (BM), CCR9<sup>+</sup>CD9<sup>+</sup>

pDCs were shown to produce high amounts of IFN- $\alpha$  following TLR9 activation (3, 4), whereas in peripheral lymph nodes, CCR9<sup>+</sup> and CCR9<sup>+</sup> pDCs were described to produce IFN- $\alpha$  (5). In contrast, Segura et al. (6) showed that splenic CCR9<sup>+</sup> pDCs produced type I IFN. Therefore, it is a matter of debate which subset is responsible for the production of type I IFN. Following stimulation of TLR7 and TLR9, pDCs also serve as a source of other cytokines and chemokines (7). It remains to be shown whether IFN- $\beta$ -producing pDCs are polyfunctional in coexpressing other immune effector molecules.

The present study clarifies that the attribute “professional type I IFN-producing cells” in the spleen following TLR9 stimulation has to be restricted to a distinct functional subset of pDCs that selectively facilitate T cell recruitment and activation.

## Materials and Methods

### Mice and in vivo treatment and infections

C57BL/6N (B6), IFNAR1<sup>-/-</sup>, IFN $\beta$ <sup>mob/mob</sup>, and IFNAR1<sup>-/-</sup>IFN $\beta$ <sup>mob/mob</sup> mice were kept under pathogen-free conditions, and experiments were approved by the government of North-Rhine Westphalia. Where indicated, mice were infected i.p. with  $2 \times 10^5$  murine CMV (MCMV) (C3X) or injected i.v. with 10  $\mu$ g CpG 1668 (TIB MOLBIOL) complexed to DOTAP (Roche) for 6 h, or as indicated.

### Generation and stimulation of BM-derived pDCs

BM-derived Flt3L-cultured pDCs were generated as previously described (8). For stimulation, CpG 1668 complexed to DOTAP (6  $\mu$ g/ml; TIB MOLBIOL) was added for 6 h, or as indicated. Surface marker expression was analyzed by FACS (Supplemental Fig. 1A).

### Flow cytometry and cell sorting

Cells were analyzed on a FACSCanto II (BD). DAPI was added for dead cell discrimination. FACS sorting was performed on a FACSARIA (BD) after MACS (Miltenyi Biotec) depletion of CD3e/CD19<sup>+</sup> cells. Abs against B220, CD3e, CD4, CD8, CD11b, CD11c, CD19, CD86, CD16/32, Ly6C, and NK1.1

<sup>\*</sup>Institute of Medical Microbiology and Hospital Hygiene, University of Düsseldorf, 40225 Düsseldorf, Germany; <sup>†</sup>Center for Biological and Medical Research, University of Düsseldorf, 40225 Düsseldorf, Germany; <sup>‡</sup>Department of Psychiatry, University of Münster, 48149 Münster, Germany; and <sup>§</sup>Cluster of Excellence EXC 1003, Cells in Motion, 48149 Münster, Germany

<sup>1</sup>J.B. and R.J.D. contributed equally to this work.

ORCID: 0000-0002-9706-4590 (A.S.); 0000-0002-9707-8191 (S.S.).

Received for publication March 13, 2015. Accepted for publication March 29, 2016.

This work was supported by the Deutsche Forschungsgemeinschaft (SCHE692/3-1, SCHE692/4-1) and the Strategic Research Fund of the University of Düsseldorf (to S.S.).

The microarray data presented in this article have been submitted to the Gene Expression Omnibus under accession number GSE68788.

Address correspondence and requests to Prof. Stefanie Scheu, Institute of Medical Microbiology and Hospital Hygiene, University of Düsseldorf, Universitätsstrasse 1, 40225 Düsseldorf, Germany. E-mail address: stefanie.scheu@hhu.de

The online version of this article contains supplemental material.

Abbreviations used in this article: B6, C57BL/6N; BM, bone marrow; MCMV, murine CMV; MONA, multilevel ontogeny analysis; pDC, plasmacytoid dendritic cell; qRT-PCR, quantitative RT-PCR.

Copyright © 2016 by The American Association of Immunologists, Inc. 0022-1767/16/\$30.00

were purchased from BD, SiglecH and mPDCA-1 were purchased from Miltenyi Biotec, CD9 (MZ3) was purchased from BioLegend, and CCR9 (eBioCW-1.2) was purchased from eBioscience.

#### Tissue preparation, cytopins, and immunohistochemistry

Spleen sections were stained as described (8). Cytopins were performed on a Cellspin II centrifuge (Tharmac) and stained using the Hemacolor rapid staining kit (Merck). Images were taken on an LSM 780 (Zeiss), Axioskop 40 (Zeiss), or Eclipse TE 2000 (Nikon) microscope with a digital camera (CCD-1300; Vosskuhler) and processed using Adobe Photoshop and ZEN 2011/12 software.

#### pDC migration and leukocyte-recruitment assays

BM-derived CpG-stimulated pDCs were sorted for IFN $\beta$ /YFP expression. Chemotaxis toward CCL19 and CCL21 (500 ng/ml; R&D Systems) was addressed using Transwell inserts with 5  $\mu$ m pore size (Corning) and the CellTiter-Glo Luminescent Cell Viability Assay (Promega). A total of  $5 \times 10^5$  IFN $\beta$ /YFP $^+$  or IFN $\beta$ /YFP $^-$  pDCs was allowed to migrate for 4 h at 37°C. For the recruitment of leukocytes, B6 mice were injected i.p. with  $2.5$ – $5 \times 10^5$  sorted IFN $\beta$ /YFP $^+$  or IFN $\beta$ /YFP $^-$  BM-derived pDCs.

#### Gene-expression analyses

RNA was isolated from ex vivo FACS-sorted pDCs using the mirVana miRNA Isolation Kit (Ambion) and hybridized to Agilent Whole Mouse Genome Oligo Microarrays ( $4 \times 44$ K). Rosetta normalization and log2 transformation were performed. Pairwise comparison of IFN $\beta$ /YFP $^+$  and IFN $\beta$ /YFP $^-$  pDCs was performed using the Rosetta Resolver. Ratios were calculated by dividing sample signal intensity by control signal intensity. The normalization that was applied is based on the Rosetta error model (9). The  $p$  value is calculated from  $X$  dev, which takes into consideration the log(Ratio) and log(Error).  $X$  dev =  $\text{Log(Ratio)/Log(Error)}$ .  $p$  value =  $1 - \text{Erf}(|X \text{ dev}|/\sqrt{2})$ .

Microarray data are available under Gene Expression Omnibus Series accession number GSE68788 (<http://www.ncbi.nlm.nih.gov/geo/query/acc.cgi?acc=GSE68788>). Significant ( $p \leq 0.01$ ) and  $>2$ -fold differentially regulated genes were subjected to multilevel ontology analysis (MONA) within the section "biological process" of this online tool and summarized to superordinate terms (<http://mips.helmholtz-muenchen.de/mona/index.aspx>). Quantitative RT-PCR (qRT-PCR) was performed using the TaqMan Master Kit with the Universal Probe Library Set (Roche) or the MESA GREEN qPCR MasterMix Plus (Eurogentec) on an iQ5 or CFX96 (Bio-Rad). The primer sequences used are shown in Supplemental Table 1.

#### Statistical analysis

Data are given as mean  $\pm$  SD, Student  $t$  tests were used, and one representative of at least independent experiments with at least three mice/group is shown, unless stated otherwise.

## Results and Discussion

### Splenic CCR9 $^+$ CD9 $^-$ pDCs secrete IFN- $\beta$ after MCMV infection or TLR9 stimulation

Because the identity of IFN- $\beta$  producers within the pDC population remains controversial, we sought to determine which specific subset of splenic pDCs is responsible for the early IFN- $\beta$  production. For this we used the unbiased in vivo approach of IFN $\beta$ /YFP reporter mice in MCMV infection or stimulation with the synthetic TLR9 ligand CpG (8). The majority of IFN $\beta$ /YFP $^+$  cells within the spleen expressed the cell surface markers CD11c, mPDCA-1, and B220 (Fig. 1A), in line with earlier reports that pDCs are the primary source of IFN- $\beta$  after MCMV infection or TLR9 activation (8, 10, 11). IFN $\beta$ /YFP expression was restricted to  $\sim 5\%$  ( $4.62 \pm 0.7\%$  [mean  $\pm$  SEM]) of all pDCs after TLR9 activation, as determined by flow cytometry (Fig. 1B). Dose-titration experiments indicated that the low frequencies of IFN $\beta$ /YFP $^+$  cells are not a linear reflection of the stimulus strength (Supplemental Fig. 1B, 1C). CD86 was upregulated on IFN $\beta$ /YFP $^+$  and IFN $\beta$ /YFP $^-$  pDCs following TLR9 stimulation or MCMV infection, indicating that both cell subsets are capable of being activated (Fig. 1C, Supplemental Fig. 1D, 1E). Therefore,

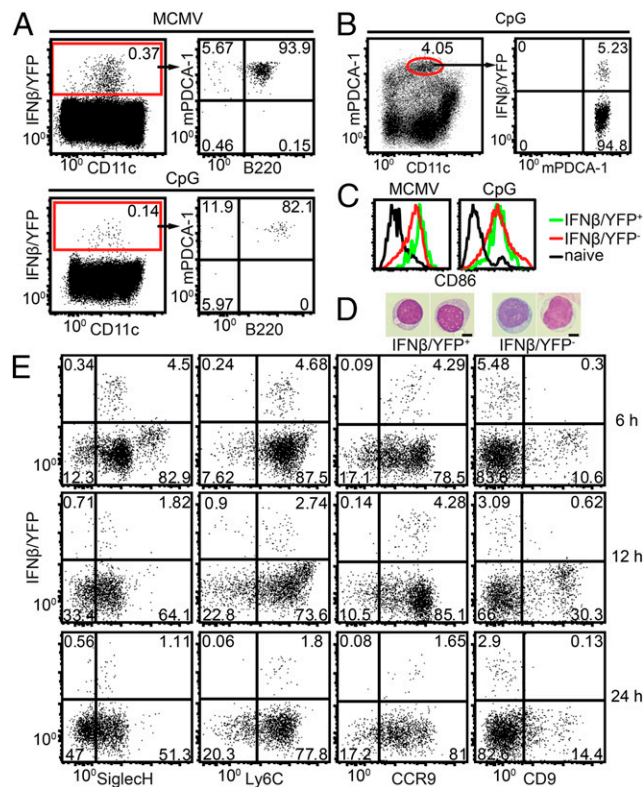


**FIGURE 1.** IFN- $\beta$  expression is restricted to a low-frequency subset of splenic CCR9 $^+$ CD9 $^-$  pDCs after MCMV infection or TLR9 stimulation. (A) IFN $\beta$ /YFP expression in splenic CD11c $^{\text{int}}$ mPDCA-1 $^+$ B220 $^+$  pDCs in IFN $\beta^{\text{mob/mob}}$  mice 6 h after MCMV infection or CpG injection. (B) Percentages of IFN $\beta$ /YFP $^+$  cells within CD11c $^{\text{int}}$ mPDCA-1 $^+$  splenic pDCs after CpG injection. (C) CD86 expression on IFN $\beta$ /YFP $^+$  pDCs and IFN $\beta$ /YFP $^-$  pDCs in comparison with pDCs of untreated mice was determined 6 h after MCMV infection or CpG injection. (D) Cytopins of ex vivo-sorted pDCs after CpG administration. Scale bars, 2  $\mu$ m. (E) Expression of IFN $\beta$ /YFP was analyzed in comparison with pDC surface markers in splenocytes at the indicated time points after CpG stimulation. Cells were pregated on living CD3 $\epsilon^+$ CD19 $^-$  cells (A and B) or additionally on CD11c $^{\text{int}}$ mPDCA-1 $^+$ (C) or CD11c $^{\text{int}}$ mPDCA-1 $^+$ CD11b $^-$  cells (D and E). See Supplemental Fig. 1F for gating.

IFN- $\beta$  expression is restricted to only a small fraction of pDCs in vivo, despite similar activation of the overall pDC population. Differences in activation marker expression observed after MCMV infection (Supplemental Fig. 1E) point to a specific influence of the virus on CD86 expression on IFN $\beta$ /YFP $^-$  pDCs. Also, insufficient activation of IFN $\beta$ /YFP $^-$  pDCs cannot be excluded in the case of the more complex virus infection. IFN $\beta$ /YFP $^+$  and IFN $\beta$ /YFP $^-$  pDCs exhibited the typical plasmacytoid morphology with a round and smooth cellular body and excentered nucleus (Fig. 1D). Splenic IFN $\beta$ /YFP $^+$  pDCs expressed the pDC markers mPDCA-1, B220, SiglecH, and Ly6C (Fig. 1A, 1E). Furthermore, the majority of IFN- $\beta$ -producing pDCs stably expressed CCR9, but not CD9, for  $\geq 24$  h after stimulation (Fig. 1E). Taken together, although IFN- $\beta$ -producing and nonproducing pDCs in the spleen upregulate surface activation markers to the same extent after CpG stimulation, IFN- $\beta$  expression is restricted to a low-frequency subset of all pDCs. Furthermore, this subset expresses CCR9 but not CD9. Our data are supported by earlier findings demonstrating that CCR9 $^-$  cells within the spleen represent precursors of conventional dendritic cells rather than bona fide pDCs (6).



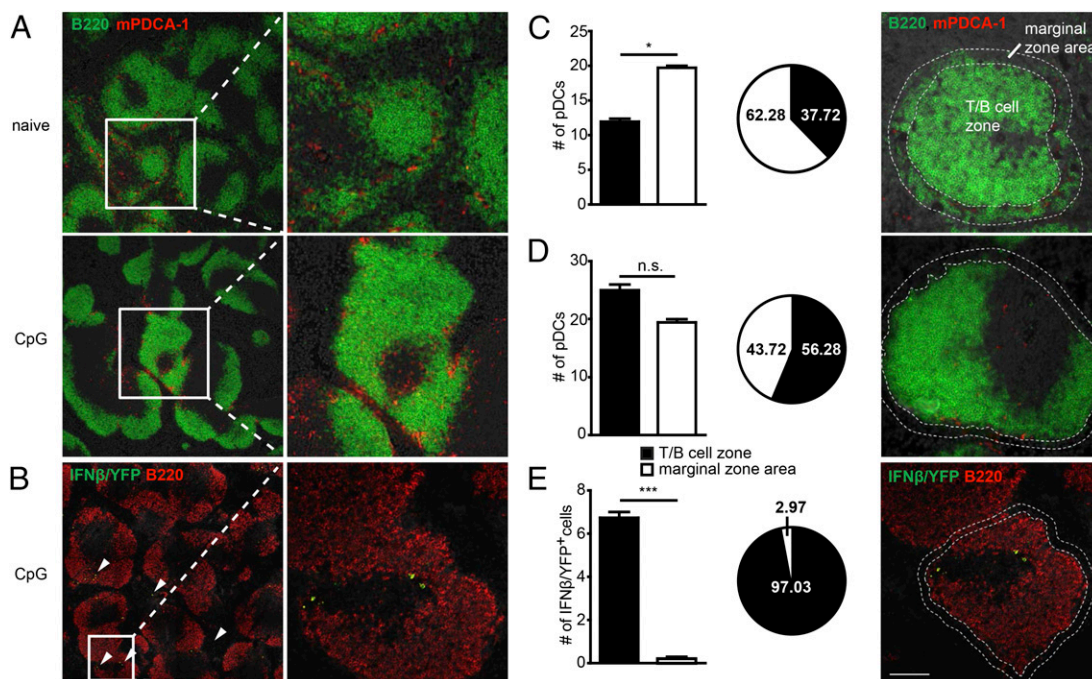


**FIGURE 2.** Differential localization of IFN- $\beta$ -producing pDCs within the splenic microarchitecture. (**A** and **B**) Immunofluorescence of the spleen of naive or CpG-stimulated B6 or IFN $\beta^{\text{mob}/\text{mob}}$  mice. Arrowheads denote exemplary IFN $\beta$ /YFP<sup>+</sup> cells. Distribution of pDCs in naive mice (**C**) and CpG-stimulated mice (**D**) and of IFN $\beta$ /YFP<sup>+</sup> cells in CpG-stimulated mice (**E**) within the T and B cell zone and the marginal zone (dotted lines). Cell counts are shown as absolute numbers (bar graphs) or the percentage distribution (pie charts) per white pulp area ( $n = 17$ – $20$ ). Original magnification  $\times 4$  (**A**, **C**, and **D**). Scale bar, 100  $\mu\text{m}$  (**B** and **E**). \* $p < 0.05$ , \*\*\* $p < 0.005$ . n.s., not significant.

Controversial reports on CCR9 and CD9 expression levels on type I IFN-producing pDCs point to organ-specific differences in pDC populations (3, 4, 6). Alternatively, the capacity to produce type I IFN might be differentially regulated, depending on the developmental stage of pDCs (4).

#### IFN $\beta$ /YFP<sup>+</sup> pDCs localize to splenic T and B cell zones

We investigated whether IFN- $\beta$ -producing pDCs localize to specific anatomical sites within the splenic microarchitecture. In naive mice,  $\sim 60\%$  of all pDCs were located within the marginal zone (Fig. 2A, 2C). Following CpG stimulation, pDCs formed clusters, as reported previously (12, 13), and were distributed equally between the T and B cell zone and the marginal zone (Fig. 2A, 2D). In marked contrast,  $>97\%$  of IFN $\beta$ /YFP<sup>+</sup> pDCs were located within T and B cell zones

(Fig. 2B, 2E). Our data demonstrate that IFN- $\beta$ -producing pDCs show a specific distribution pattern within the spleen rather than being randomly interspersed within the overall splenic pDC population.

#### A specific immune-activating gene-expression signature characterizes IFN- $\beta$ -expressing pDCs

We next asked whether these IFN- $\beta$ -producing pDCs harbor further specialized functional properties associated with a specific gene-expression profile. Splenic CD11c<sup>int</sup>mPDCA-1<sup>+</sup> CD11b<sup>−</sup> pDCs were sorted by FACS 6 h after CpG administration into IFN $\beta$ /YFP<sup>−</sup> and IFN $\beta$ /YFP<sup>+</sup> populations (Supplemental Fig. 1G). Microarray analyses defined 1446 genes as significantly ( $p \leq 0.01$ ) and  $>2$ -fold over- or underrepresented in IFN $\beta$ /YFP<sup>+</sup> pDCs versus IFN $\beta$ /YFP<sup>−</sup> pDCs (Fig. 3A).

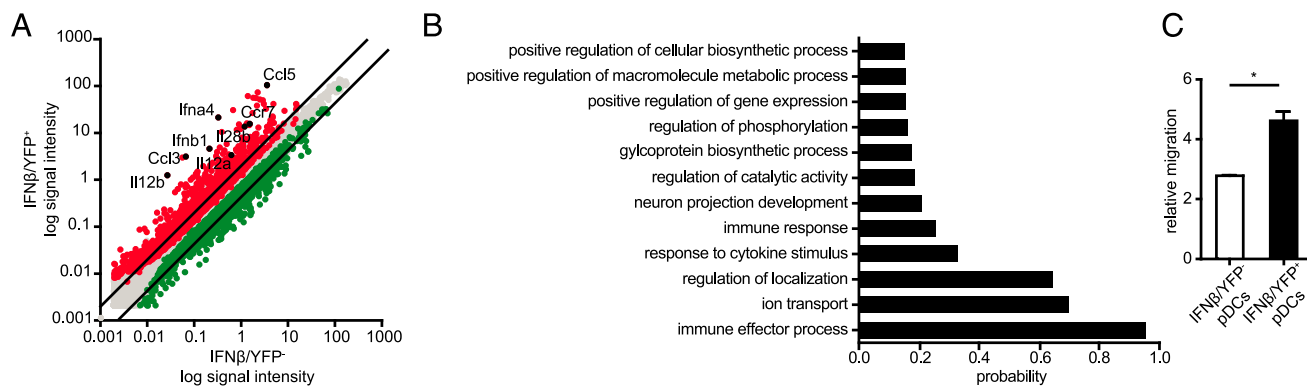


**FIGURE 3.** IFN- $\beta$ -producing pDCs harbor a proinflammatory gene-expression profile. (**A**) Pairwise comparison of the log signal intensities for transcripts, as analyzed by microarray. Red and green dots represent genes differentially expressed in IFN $\beta$ /YFP<sup>+</sup> and IFN $\beta$ /YFP<sup>−</sup> pDCs, respectively. (**B**) MONA for overrepresented genes in IFN $\beta$ /YFP<sup>+</sup> versus IFN $\beta$ /YFP<sup>−</sup> pDCs. (**C**) Transwell migration assay of CpG-activated BM-derived IFN $\beta$ /YFP<sup>+</sup> and IFN $\beta$ /YFP<sup>−</sup> pDCs in response to CCL19 and CCL21. Shown is one representative of two independent experiments. \* $p < 0.05$ .

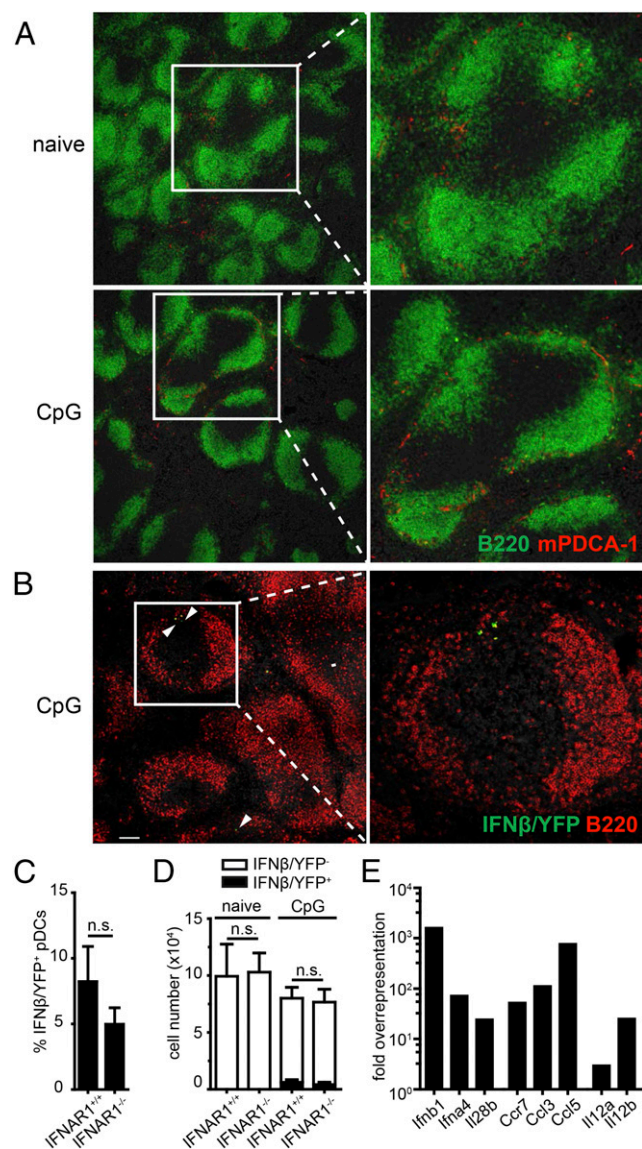


**FIGURE 4.** IFNAR1 deficiency does not affect the functional properties of IFN- $\beta$ -producing splenic pDCs after CpG stimulation. (A and B) Immunofluorescence of the spleen of naive and CpG-stimulated IFNAR1<sup>-/-</sup> IFN $\beta$ <sup>mob/mob</sup> mice. Arrowheads point to exemplary IFN $\beta$ /YFP<sup>+</sup> cells. Original magnification  $\times 4$  (A). Scale bar, 100  $\mu$ m (B). Percentages of IFN $\beta$ /YFP<sup>+</sup> cells (C) and total numbers of IFN $\beta$ /YFP<sup>+</sup> and IFN $\beta$ /YFP<sup>-</sup> pDCs (D) gated on CD11c<sup>int</sup>mPDCA-1<sup>+</sup> pDCs after CpG injection, as assayed by flow cytometry. (E) qRT-PCR shown as fold overrepresentation in IFN $\beta$ /YFP<sup>+</sup> versus IFN $\beta$ /YFP<sup>-</sup> pDCs sorted from IFNAR1<sup>-/-</sup> IFN $\beta$ <sup>mob/mob</sup> mice. n.s., not significant.

The classical pDC surface marker mPDCA-1 and hallmark transcription factor E2-2 (2) did not exhibit significantly different expression levels in IFN $\beta$ /YFP<sup>+</sup> and IFN $\beta$ /YFP<sup>-</sup> pDCs. Several genes associated with TLR9 stimulation were expressed similarly in IFN $\beta$ /YFP<sup>+</sup> and IFN $\beta$ /YFP<sup>-</sup> pDCs compared with naive pDCs (Supplemental Fig. 1H). In contrast, IFN- $\beta$ , other type I IFNs, the type III IFN Il28b, Th cell-differentiation cytokines (e.g., Il12b and Il12a), and genes involved in chemotaxis (e.g., CCL3, CCL5, and CCR7) were among the highest overrepresented genes in IFN $\beta$ /YFP<sup>+</sup> pDCs. This was confirmed by independent qRT-PCR analyses (Supplemental Fig. 1I). Of note, expression changes in these genes were observed in IFN $\beta$ /YFP<sup>+</sup> pDCs versus IFN $\beta$ /YFP<sup>-</sup> pDCs, as well as in IFN $\beta$ /YFP<sup>+</sup> pDCs and IFN $\beta$ /YFP<sup>-</sup> pDCs

versus naive pDCs (Supplemental Fig. 1J). To fully clarify the relative differentiation and activation status of IFN $\beta$ /YFP<sup>+</sup> pDCs and IFN $\beta$ /YFP<sup>-</sup> pDCs versus naive pDCs, future experiments (e.g., direct comparisons of the transcriptome and proteome of these three groups) will be needed. MONA identified genes involved in immune effector processes and regulation of localization as active specifically in IFN- $\beta$ -producing pDCs (Fig. 3B). In line with the differential expression of CCR7, IFN $\beta$ /YFP<sup>+</sup> pDCs exhibited a greater migration toward CCL19 and CCL21 compared with IFN $\beta$ /YFP<sup>-</sup> pDCs (Fig. 3C), which correlated with their specific localization within the splenic white pulp. This further indicates that IFN $\beta$ /YFP<sup>+</sup> pDCs are a specialized subset that is highly capable of efficiently producing IFN- $\beta$ .

#### Expression profile and localization of IFN- $\beta$ -producing pDCs are independent of type I IFN signaling

Following TLR9 activation of IFNAR1<sup>-/-</sup> mice, the majority of IFN- $\beta$ -producing pDCs were located within the splenic T and B cell zones, similar to their localization in IFNAR1<sup>+/+</sup> animals (Figs. 2A, 2B, 4A, 4B). Furthermore, no significant differences in the percentages or absolute numbers of total and IFN $\beta$ /YFP<sup>+</sup> pDCs were observed between IFNAR1<sup>+/+</sup> and IFNAR1<sup>-/-</sup> mice after CpG stimulation (Fig. 4C, 4D), in line with previous studies demonstrating that type I IFN production by pDCs occurred independently of the IFNAR-mediated feedback loop (14). Also, IFN- $\beta$  serum levels were similar in IFNAR1<sup>+/+</sup> and IFNAR1<sup>-/-</sup> mice, whereas IFN- $\alpha$  levels were reduced in the absence of IFNAR1 (Supplemental Fig. 1K, 1L). To elucidate a possible involvement of type I IFN signaling in the specific gene-expression signature in IFN- $\beta$ -producing pDCs, we isolated IFN $\beta$ /YFP<sup>+</sup> or IFN $\beta$ /YFP<sup>-</sup> pDCs from IFNAR1<sup>-/-</sup> IFN $\beta$ <sup>mob/mob</sup> mice by FACS and subsequently performed qRT-PCR on selected genes (Fig. 4E). The expression profile of selected immune-response genes was comparable to that of IFN- $\beta$ -producing pDCs from IFNAR1<sup>+/+</sup> mice, demonstrating that, independent of IFNAR-mediated signaling, IFN- $\beta$ -producing pDCs are equipped with an intrinsic and specialized gene-expression profile for the effective orchestration of cellular immune responses.

#### IFN- $\beta$ -producing pDCs control immune effector cell recruitment

The gene-expression signature of IFN- $\beta$ -producing pDCs demonstrates that these cells produce a broad range of type I IFNs and proinflammatory cytokines, as well as express CCL3 and CCL5 capable of promoting the recruitment of NK cells and CD4<sup>+</sup> and CD8<sup>+</sup> T cells. In an in vivo model in which naive untreated pDCs or sorted CpG-stimulated IFN $\beta$ /YFP<sup>+</sup> or IFN $\beta$ /YFP<sup>-</sup> pDCs were injected i.p. into wild-type mice,

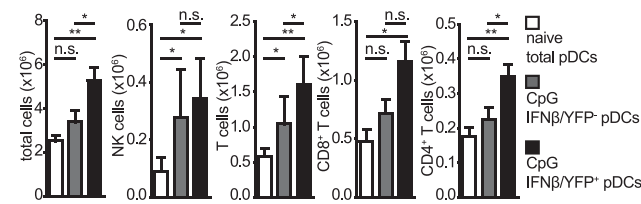


**FIGURE 5.** Enhanced chemotactic properties of IFN- $\beta$ -producing pDCs. B6 mice were injected i.p. with BM-derived untreated pDCs or CpG-stimulated IFN $\beta$ /YFP<sup>+</sup> or IFN $\beta$ /YFP<sup>-</sup> pDCs. FACS analysis of peritoneal exudates at 72 h postinfection from one representative of two independent experiments. \* $p$  < 0.05, \*\* $p$  < 0.01. n.s., not significant.

IFN $\beta$ /YFP<sup>+</sup>, but not IFN $\beta$ /YFP<sup>−</sup>, pDCs promoted the influx of greater absolute numbers of total cells into the peritoneal cavity compared with naive pDCs (Fig. 5). This differential recruitment ability pertained to CD8<sup>+</sup> and CD4<sup>+</sup> T cells, whereas no significant differences were noted with regard to NK cells (Fig. 5).

In this study, we identified a functionally distinct subset of IFN- $\beta$ -producing pDCs with enhanced migratory capacity capable of mediating cellular immune responses. Our results indicate that, after systemic activation of TLR9, only a small subset of pDCs was responsible for the initial expression of type I IFNs in the antiviral response. The IFN- $\beta$ -producing pDCs were strategically located within the T cell zone of the splenic white pulp and were equipped with a specific gene signature profile enabling them to control leukocyte recruitment and coordinate early cellular immune responses. These findings cast doubt on current models suggesting a stochastic expression of IFN- $\beta$  (15, 16). A possible explanation for the differential regulation of IFN- $\beta$  expression is an epigenetic blockade of the IFN- $\beta$  promoter in non-IFN- $\beta$ -producing pDCs, as described for mouse embryonic fibroblasts (17). None of the functions described above were dependent on IFNAR-mediated signaling but represented cell-intrinsic properties of these natural type I IFN-producing cells. These findings have to be taken into consideration in the design and interpretation of vaccination and therapy approaches involving pDC-based strategies in infectious and antitumor immunology, as well as autoimmunity.

## Acknowledgments

We thank S. Kropp for technical assistance and T. Klitz for animal husbandry.

## Disclosures

The authors have no financial conflicts of interest.

## References

- Gilliet, M., W. Cao, and Y. J. Liu. 2008. Plasmacytoid dendritic cells: sensing nucleic acids in viral infection and autoimmune diseases. *Nat. Rev. Immunol.* 8: 594–606.
- Reizis, B., A. Bunin, H. S. Ghosh, K. L. Lewis, and V. Sisirak. 2011. Plasmacytoid dendritic cells: recent progress and open questions. *Annu. Rev. Immunol.* 29: 163–183.
- Björck, P., H. X. Leong, and E. G. Engleman. 2011. Plasmacytoid dendritic cell dichotomy: identification of IFN- $\alpha$  producing cells as a phenotypically and functionally distinct subset. *J. Immunol.* 186: 1477–1485.
- Schlitzer, A., J. Loschko, K. Mair, R. Vogelmann, L. Henkel, H. Einwächter, M. Schiemann, J. H. Niess, W. Reindl, and A. Krug. 2011. Identification of CCR9<sup>+</sup> murine plasmacytoid DC precursors with plasticity to differentiate into conventional DCs. *Blood* 117: 6562–6570.
- Hadeiba, H., T. Sato, A. Habtezion, C. Oderup, J. Pan, and E. C. Butcher. 2008. CCR9 expression defines tolerogenic plasmacytoid dendritic cells able to suppress acute graft-versus-host disease. *Nat. Immunol.* 9: 1253–1260.
- Segura, E., J. Wong, and J. A. Villadangos. 2009. Cutting edge: B220+CCR9<sup>+</sup> dendritic cells are not plasmacytoid dendritic cells but are precursors of conventional dendritic cells. *J. Immunol.* 183: 1514–1517.
- Swiecki, M., and M. Colonna. 2010. Unraveling the functions of plasmacytoid dendritic cells during viral infections, autoimmunity, and tolerance. *Immunity. Rev.* 234: 142–162.
- Scheu, S., P. Dresing, and R. M. Locksley. 2008. Visualization of IFN $\beta$  production by plasmacytoid versus conventional dendritic cells under specific stimulation conditions in vivo. *Proc. Natl. Acad. Sci. USA* 105: 20416–20421.
- Weng, L., H. Dai, Y. Zhan, Y. He, S. B. Stepaniants, and D. E. Bassett. 2006. Rosetta error model for gene expression analysis. *Bioinformatics* 22: 1111–1121.
- Kumagai, Y., O. Takeuchi, H. Kato, H. Kumar, K. Matsui, E. Morii, K. Aozasa, T. Kawai, and S. Akira. 2007. Alveolar macrophages are the primary interferon- $\alpha$  producer in pulmonary infection with RNA viruses. *Immunity* 27: 240–252.
- Zucchini, N., G. Bessou, S. H. Robbins, L. Chasson, A. Raper, P. R. Crocker, and M. Dalod. 2008. Individual plasmacytoid dendritic cells are major contributors to the production of multiple innate cytokines in an organ-specific manner during viral infection. *Int. Immunol.* 20: 45–56.
- Asselin-Paturel, C., G. Brizard, K. Chemin, A. Boonstra, A. O'Garra, A. Vicari, and G. Trinchieri. 2005. Type I interferon dependence of plasmacytoid dendritic cell activation and migration. *J. Exp. Med.* 201: 1157–1167.
- Blasius, A., W. Vermi, A. Krug, F. Facchetti, M. Cella, and M. Colonna. 2004. A cell-surface molecule selectively expressed on murine natural interferon-producing cells that blocks secretion of interferon- $\alpha$ . *Blood* 103: 4201–4206.
- Barchet, W., M. Cella, B. Odermatt, C. Asselin-Paturel, M. Colonna, and U. Kalinke. 2002. Virus-induced interferon  $\alpha$  production by a dendritic cell subset in the absence of feedback signaling in vivo. *J. Exp. Med.* 195: 507–516.
- Apostolou, E., and D. Thanos. 2008. Virus Infection Induces NF- $\kappa$ B-dependent interchromosomal associations mediating monoallelic IFN- $\beta$  gene expression. *Cell* 134: 85–96.
- Zhao, M., J. Zhang, H. Phatnani, S. Scheu, and T. Maniatis. 2012. Stochastic expression of the interferon- $\beta$  gene. *PLoS Biol.* 10: e1001249.
- Fang, T. C., U. Schaefer, I. Mecklenbrauker, A. Stienen, S. Dewell, M. S. Chen, I. Rioja, V. Parravicini, R. K. Prinjha, R. Chandwani, et al. 2012. Histone H3 lysine 9 dimethylation as an epigenetic signature of the interferon response. *J. Exp. Med.* 209: 661–669.